J Biochem Tech (2016) 7(3): 1069-1077
ISSN: 0974-2328

Isolation, screening and identification of fungal organisms for biosorption of fluoride: Kinetic study and statistical optimization of biosorption parameters

Poornima G. Hiremath, Navya P.N., Vivek Chandramohan, Thomas Theodore*

Received: 11 April 2016 / Received in revised form: 06 October 2016, Accepted: 08 October 2016, Published online: 11 October 2016

Abstract

Fluoride contamination in groundwater has raised serious health concerns. The traditional technologies available for fluoride removal are having several shortcomings. Hence, biosorption is considered as a potential eco-friendly alternative to the existing methods. In the present work, several soil samples were collected from different fluoride contaminated regions of Pavagada taluk, Tumkur district, Karnataka, India. These samples were used as a source to isolate fungi with distinct morphological characteristics. The four fluoride-resistant fungal species were identified as *Penicillium camemberti* SIT-CH-1, *Aspergillus ficuum* SIT-CH-2, *Aspergillus terreus* SIT-CH-3, and *Aspergillus flavipes* SIT-CH-4 and were tested for their biosorption properties. The interative effect of parameters such as initial fluoride concentration, pH, contact time, and biosorbent dosage were studied using Central Composite design (CCD) of Response Surface Methodology (RSM). *Penicillium camemberti* SIT-CH-1 showed better fluoride removal than the other three fungal species. The pseudo-second order kinetic model provided the best fit for all the four fungal species for fluoride biosorption.

Keywords: Fluoride, Biosorption, Fungal species, RSM, CCD.

Introduction

Fluoride is toxic and non-biodegradable, which magnifies in the environment due to bioaccumulation through the food chain. Due to severe health problems caused by excess fluoride, the World Health Organization (WHO) has set 1.5 mg/L as the permissible limit of fluoride content in drinking water (WHO 2008). India, Sri Lanka, China, Africa, and Turkey are some of the many countries facing the problem of high fluoride concentrations in groundwater. A number of studies have been conducted for the removal of fluoride from water. The traditional methods of removing fluoride have several disadvantages. Chemical precipitation produces large quantities of toxic sludge (Volesky B, 2001). The ion-exchange process is relatively expensive due to the high cost of synthetic ion-exchange resins.

Membrane filtration processes like reverse osmosis and nano-filtration have high efficiency but involves large installation, maintenance, and running costs (Volesky B, 2001). Other methods of fluoride removal include usage of natural materials. Biosorption using non-living biomass of algae, fungi, yeast, and bacteria (Volesky and Holan, 1995) are found to be an efficient, eco-friendly, and economical way of treating fluoride present in water. The specificity of biosorption makes it an excellent candidate for industrial applications where high volume, low concentration, complex ionic matrix waste or process solutions need to be treated for the purpose of sequestering targeted elements. Earlier, the fungus has been shown to have excellent heavy metal sorption capacity (Purvis and Halls, 1996). Hence, in the present study, the possibility of using fungal biomass for the biosorption of fluoride anion is considered. An effort has been made to isolate and screen different fluoride-resistant fungi from the fluoride-affected areas of Pavagada region. The next objective was to assess the interactive effect of pH, initial fluoride concentration, biosorbent dosage, and contact time using CCD of RSM.

Materials and Methods

Fluoride estimation

Fluoride was estimated by the Mettler Toledo fluoride ion selective electrode [perfectION™ combined fluoride electrode make] and Mettler Toledo ion analyzer [SevenCompact pH/ion meter S220 make]. Total ionic strength adjusting buffer III (TISAB – III) solution was added to both samples and standards in the ratio 1:10 to regulate the ionic strength of samples and standard solutions. Sodium fluoride was used for the preparation of a stock solution of fluoride (1000 mg L−1) by dissolving an appropriate quantity in deionized water.

Poornima G. Hiremath, Thomas Theodore*

Department of Chemical Engineering, Siddaganga Institute of Technology, Tumkur-572103, Karnataka, India

*Tel: +91-9886160440; *E-mail: theodorethomas2015@gmail.com

Navya P.N., Vivek Chandramohan,

Department of Biotechnology, Siddaganga Institute of Technology, Tumkur-572103, Karnataka, India

Sample Collection

Contaminated soil samples collected from different sites of Pavagada taluk of Tumkur district, Karnataka, India were used as a source to isolate fluoride-resistant fungi with distinct morphological colony characters. Pavagada is one of the areas in Karnataka, where high fluoride content in groundwater has been reported (Mamatha and Sudhakar Rao, 2010).

Isolation, screening, and identification of fungal organisms

The fungal organisms were isolated from the collected soil samples by the serial dilution method (Harley and Prescott, 1993). Screening of the isolates for fluoride removal was carried out on selective agar plates containing potato dextrose agar (PDA) with 20 ppm of fluoride concentration. Point inoculation was done on agar plates with pure cultures and was incubated at 30°C for 72 h. Various colonies of different morphologies were individually observed (Barnett and Hunter, 1988) and replicated on PDA plates and then kept at 4ºC for further use. After cultivation, the mycelium was separated from the liquid medium.

Genomic DNA isolation, amplification and sequencing of fungal samples was carried out using 18s Internal Transcribed Spacer's (ITS) primers. The ITS region of fungal DNA was amplified using the fungal specific primer set: ITS F (GGAAGTAAAAGTCGTAACAAGG) and ITS R (TCCTCCGCTTATTGATATGC). PCR was performed in a total volume of 50 µL and the reaction mixture contained 5 µL of 10X PCR buffer, 2 µL of dNTP mixture, 1 µL of each primer, and 1 µL of Taq polymerase, 5 µL of the template and diluted to a final volume of 35 µl with de-ionized distilled water. PCR was conducted using a thermal cycler GeneAmp PCR System 9700 (Perkin-Elmer, CA, USA) to subject the reaction mix to 35 cycles of the following reaction conditions: denaturation at 94°C for 30 s, primer annealing at 55°C for 30 s, and extension at 72°C for 1 min, followed by final extension for 7 min at 72°C to ensure full extension of the products (Vu et al. 2009). The amplified PCR products were then analyzed in 1.0% (w/v) agarose gel. Further, the PCR products were purified with a PCR products purification kit (Aristogene PCR product purification kit) and were sequenced by Aristogene Biosciences Pvt Ltd, Bangalore. To analyze the fungal species, DNA sequence of the ITS-18S rDNA related sequences were obtained from the GenBank.

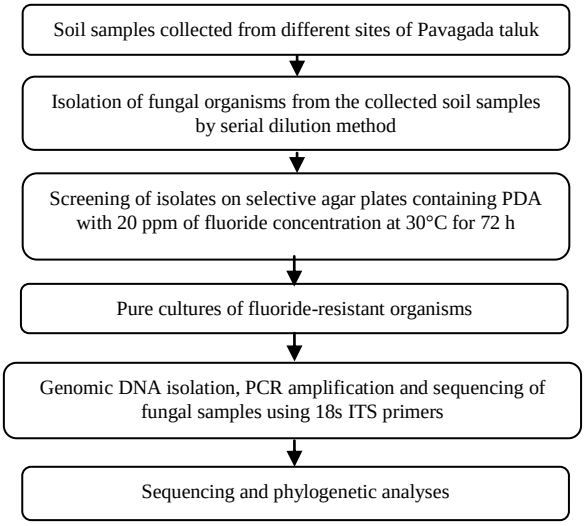

Figure 1: Flow diagram for Isolation, screening, and identification of fungal organisms

The sequence was compared with the BLAST program from the National Center for Biotechnological Information (NCBI) for the identification of the species. The organism was identified based on the highest homology of the sequence with sequence available in the database. The CLC bio package was used for all analyses (Navya and Pushpa, 2013). Figure 1 indicates the flow diagram for isolation, screening, and identification of fungal organisms.

Fungal characterization

On the basis of nucleotide homology and phylogenetic analysis, the microbes were identified as *Penicillium camemberti* SIT-CH-1, *Aspergillus ficuum* SIT-CH-2, *Aspergillus terreus* SIT-CH-3, and *Aspergillus flavipes* SIT-CH-4 (Figure 2 (a-d)). The fungal nucleotide sequences of the four species were submitted to the GenBank of NCBI. The accession numbers of the same are listed in Table 1.

Table 1. GenBank accession number of the fungal species

Species Name	Accession No.
Penicillium camemberti SIT-CH-1	KT200225
Aspergillus terreus SIT-CH-3	KT200226
Aspergillus ficuum SIT-CH-2	KT200227
Aspergillus flavipes SIT-CH-4	KT364632

Preparation of fungal biosorbents

In this study, the four fluoride-resistant fungal species were cultured in 200 mL potato dextrose broth at 30°C for 72 h and the obtained biomass was autoclaved. The fungal mats were separated, washed with distilled water, and dried in a hot air oven at 70ºC for 24 h. The dried biomass was then ground to a fine powder.

Batch sorption experiments

Experiments were carried out in 250-mL polypropylene flasks by adding the desired amount of biosorbent to the desired concentrations of fluoride solutions, pH and agitating the flasks at 190 rpm in a rotary shaker incubator for a known period of time at 30°C. The solution was then filtered using Whatman filter paper No. 42 to separate the biomass. The filtrate was analyzed for residual fluoride concentration by the fluoride ion selective electrode.

The percentage biosorption was calculated using Eq. (1):

$$\% \text{ biosorption} = \frac{(C_0 - C_e)}{C_0} * 100 \quad (1)$$

The amount of fluoride (mg) adsorbed per g of adsorbent after equilibrium (qe) was calculated using Eq. (2):

$$q_e = \frac{(C_o - C_e)V}{M} \quad (2)$$

where Co and Ce (mg/L) represent the concentrations of the fluoride ion present initially and at equilibrium in the solution, respectively. V is the volume of the solution (L) and M is the mass of adsorbent (g).

The response surface methodology were used to assess the interactive effect of pH, initial fluoride concentration, biosorbent dosage, and contact time at more levels with minimal number of experiments suggested by Central Composite Design. Design Expert Version 9.0.3.1 (Stat-Ease, Minneapolis, MN) was used to evaluate the effects

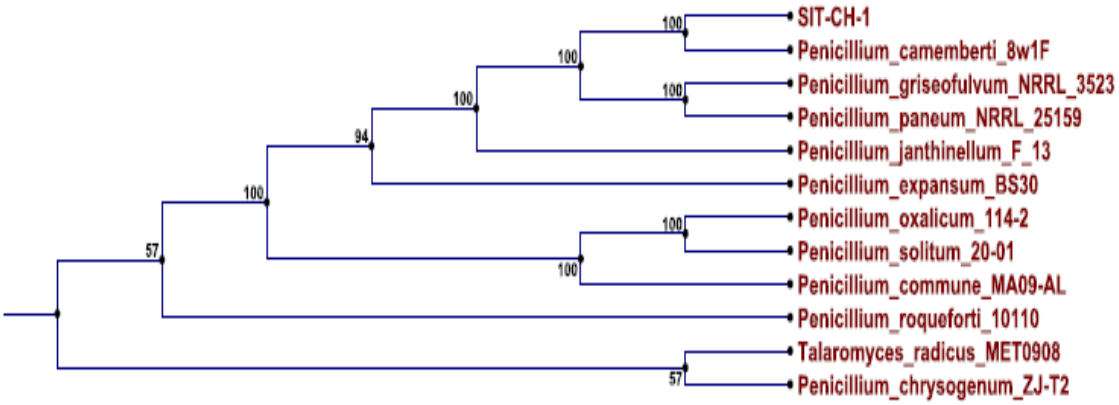

Figure 2(a)

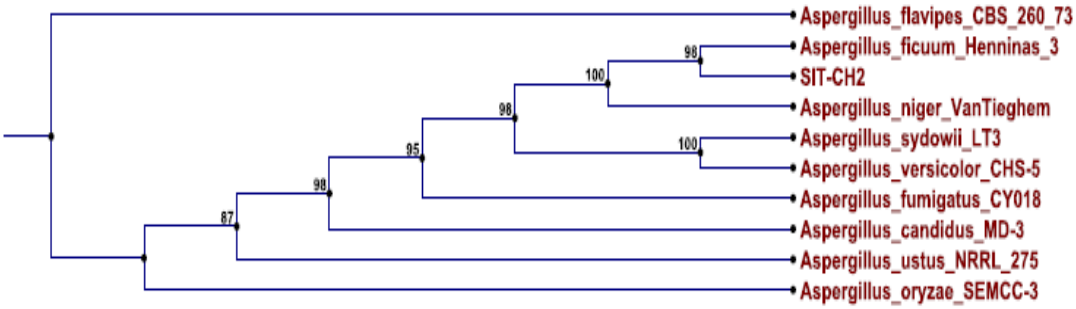

Figure 2(b)

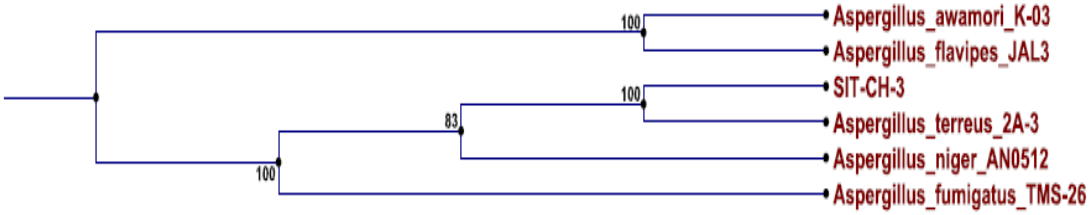

Figure 2(c)

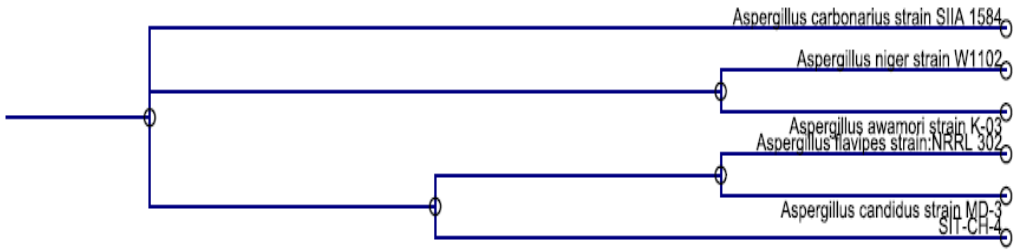

Figure 2(d)

Figure 2. Phylogenetic tree based on the ITS-18S rDNA sequence which shows the positions of the 2(a) SIT-CH-1, 2(b) SIT-CH-2, 2(c) SIT-CH-3, 2(d) SIT-CH-4 and related strains

and complex interactions of each process variable. The results were analyzed by applying the contour plots and analysis of variance (ANOVA) (Myers and Montgomery, 2002).

The quadratic equation model for predicting the optimal point was expressed according to Eq. (3):

$$Y = \beta_0 + \sum_{i}^{k} \beta_i x_i + \sum_{ii}^{k} \beta_{ii} x_i^2 + \sum_{i<j} \beta_{ij} x_i x_j \quad (3)$$

where Y is the predicted response, xi, xj refer to the independent variables and β0, βi, βii, βij are the regression coefficients.

Characterization of biosorbents

Fourier Transform Infrared (FTIR) spectra of biosorbents before and after adsorption were recorded. FTIR analyses were carried out at room temperature on Spectrum TwoTM from PerkinElmer, Waltham, MA at a resolution of 2 cm^{-1} in the wavenumber range 400 – 4000 cm^{-1} for studying the chemical groups on the surface of the fungal powder.

Determination of the amount of hydrogen per culture volume

The number of moles of hydrogen in the gas phase over 10 mL cell suspension in the closed 32 mL test tube was measured utilizing a gas chromatograph equipped with a molecular sieve column and a thermal conductivity detector (GC-320, GL science Inc.; column, Molecular sieve 13X; column temperature, 37ºC; injector temperature, 45ºC; detector temperature 80ºC) with nitrogen gas as the carrier gas. Number of moles of hydrogen per culture volume (y_{H2}) was obtained by the measured number of moles of hydrogen divided by culture volume. Gas chromatography condition of this method was previously reported (Chongsuksantikul et al. 2014).

Results and Discussion

Characterization of the biosorbents

The main functional groups present on *Penicillium camemberti* SIT-CH-1, *Aspergillus ficuum* SIT-CH-2, *Aspergillus terreus* SIT-CH-3, and *Aspergillus flavipes* SIT-CH-4 species which are responsible for biosorption of fluoride ions were found using the FTIR spectra (Smith, 1998).

Figure 3(a-d) depicts the FTIR spectra of the fungal biomass before and after fluoride biosorption. The broadband range of 3200-3500 cm^{-1} denotes the presence of N-H bond of amino groups associated with -OH groups. The relative differences in band intensity are similar to the differences in the concentrations of the respective functional groups associated with the bands. The peak around 2850 cm^{-1} is due to the presence of alkyl group (C-H) and at 1724 cm^{-1} may be due to the involvement of double bond structures such as C=C or C=O groups. The peak in the region of 1375 cm^{-1} may be attributed to N-H bending in the amine group. The band observed at 1033 cm^{-1} denotes C-O stretching of carboxylic acids. Thus, the fungal biomass is expected to possess hydroxyl, carboxyl, and amine groups on its surface as significant sorption sites (Table 2). The peaks for –NH shifted slightly in the fluoride-laden biomass. This reduction in wavenumber may indicate the interaction of $–NH_2$ groups of the biomass with fluoride ions. The hydrogen bonding in amines is weaker than that of hydroxyl groups, so $–NH_2$ stretching bands are not as broad or intense as –OH stretching bands. A slight broadening of $–NH_2$ stretching band in the fluoride biosorbed fungal biomass may be due to hydrogen bonding between the protonated amine ($–NH_3^+$) and fluoride ions (Smith, 1998). Similar results were reported by other authors while studying fluoride sorption on *Pleurotus eryngii* white-rot fungus (Amin et al. 2015). The slight broadening of the band at 3200-3500 cm^{-1} -region in the fluoride-laden biomass indicates the interaction between amine and hydroxyl groups with biomass.

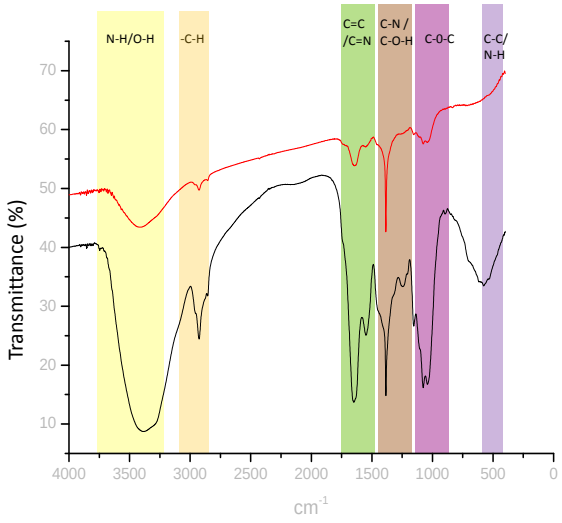

Figure 3(a)

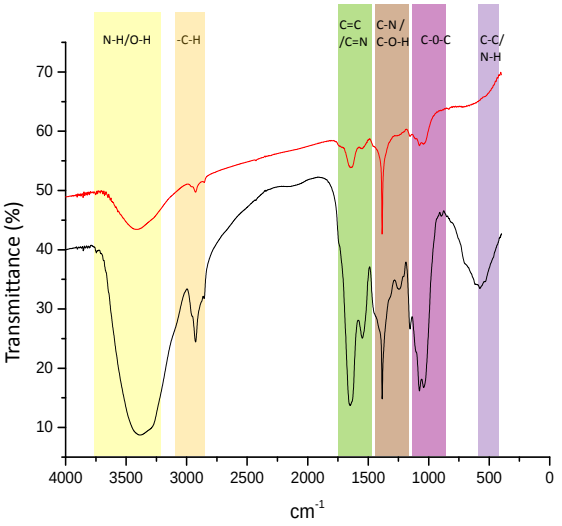

Figure 3(b)

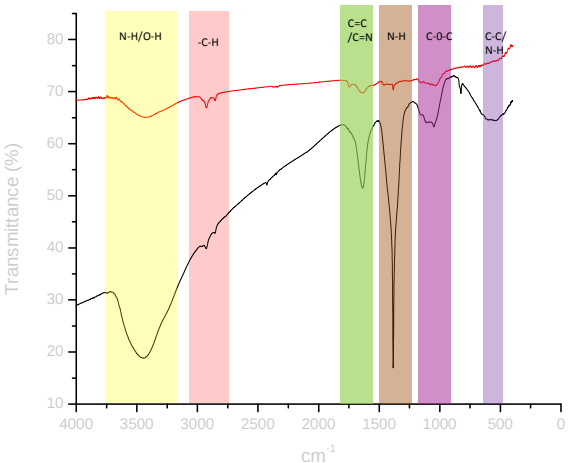

Figure 3(c)

Table 2: Surface functional groups observed on the *Penicillium camemberti* SIT-CH-1, *Aspergillus ficuum* SIT-CH-2, *Aspergillus terreus* SIT-CH-3, and *Aspergillus flavipes* SIT-CH-4 fungi biosorbents before and after biosorption

Before biosorption, cm^{-1}	After biosorption	Bands indicating functional groups
	***Penicillium camemberti* SIT-CH-1**	
3421	3391	O-H stretching; N-H stretching
2926	2927	C-H stretching
1645	1652	C=C stretching or C=N amide stretching
1385	1384	C-N deformation, C-O-H stretching
1044	1041	C-O-C asymmetrical stretching
833	833	C-C skeleton
576	577	NH torsional oscillation
	***Aspergillus ficuum* SIT-CH-2**	
3401	3430	O-H stretching; N-H stretching
2926	2926	C-H stretching, NH_3 symmetric
1646	1639	C=C stretching or C=N amide stretching
1384	1384	C-N deformation, C-O-H stretching
1076	1072	C-O-C asymmetrical stretching
854	854	C-O deformation, NH_2 rocking
603	601	C-C skeleton
	***Aspergillus terreus* SIT-CH-3**	
3436	3438	O-H stretching; N-H stretching
1639	1638	C=C stretching or C=N amide stretching
1384	1384	C-N deformation, C-O-H stretching
1052	1049	C-O-C asymmetrical stretching
828	826	C-H deformation, NH vibration
597	601	C-C skeleton
540	537	NH torsional oscillation
	***Aspergillus flavipes* SIT-CH-4**	
3421	3423	O-H stretching; N-H stretching
2927	2926	C-H stretching
2856	2855	C-H deformation
1640	1644	C=C stretching or C=N amide stretching
1384	1384	C-N deformation, C-O-H stretching
1047	1038	C-O-C asymmetrical stretching
850	839	C-O deformation, NH vibration
584	577	C-C skeleton, NH torsional oscillation

Table 3. Adsorption kinetic parameters for the fluoride removal by four fungal biosorbents

Adsorption Kinetic Model	*Penicillium camemberti* SIT-CH-1	*Aspergillus ficuum* SIT-CH-2	*Aspergillus terreus* SIT-CH-3	*Aspergillus flavipes* SIT-CH-4
Pseudo-first-order model				
Rate Constant, K_1 (min^{-1})	11.48	9.29	3.80	3.17
Constants, q_1(mg/g)	1.94	3.48	2.42	2.58
R^2	0.7177	0.847	0.67	0.76
Pseudo-second-order model				
Rate Constant, K_2 (g/mg.min)	0.01	0.014	0.033	0.05
Constant, q_2(mg/g)	2.51	3.88	2.65	2.73
R^2	0.961	0.996	0. 9952	0.998
Intra-particle diffusion model				
Rate Constant, Kp ($mg/g.min^{1/2}$)	0.099	0.12	0.05	0.043
Constant, C	0.69	1.76	1.76	2.01
R^2	0.96	0.989	0.9753	0.997
Elovich model				
Rate Constant, α (mmole/g.min)	2.12	6.72	2862.8	49234.2
Constant, β (g/mmole)	0.39	0.53	0.21	0.181
R^2	0.8643	0.974	0.8914	0.958

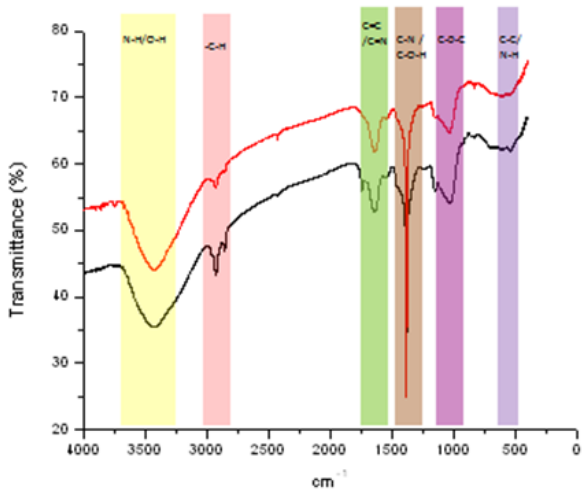

Figure 3(d)

Figure 3. FTIR spectra of fungal biomass and fluoride treated 3(a) *Penicillium camemberti* SIT-CH-1, 3(b) *Aspergillus ficuum* SIT-CH-2, 3(c) *Aspergillus terreus* SIT-CH-3 and 3(d) *Aspergillus flavipes* SIT-CH-4 fungal biomass at pH 2 (— Before adsorption,— After adsorption)

Kinetics of sorption

In this study, four different kinetic models (Pseudo-first order, Pseudo-second order, Elovich, and Intra-particle diffusion) were used to predict the biosorption kinetics of fluoride on fungal biosorbents.

In order to obtain the data of concentration of fluoride versus time, samples of solution were withdrawn at regular intervals of time (10, 20, 30, 60, 120, 180, 240 and 300 min) during biosorption and analyzed for fluoride after separation of biomass by filtration.

The pseudo-first order rate equation is given by Eq. (4) (Lagergren, 1898):

$$\ln(q_e-q_t) = \ln(q_e) - k_1 t \quad (4)$$

where qe and qt are the amounts of fluoride adsorbed (mg/g) at equilibrium and at time t (min), respectively, and k_1 (L/min) is the adsorption rate constant of first order adsorption. A straight line of $\ln(q_e-q_t)$ versus t suggests the applicability of this kinetic model. qe and k1 were determined from the intercept and slope of the plot.
In addition, the experimental data was also applied to the pseudo-second order kinetic model Eq. (5) (Ho and Mckay, 1999):

$$\frac{t}{q_t} = \frac{1}{k_2 q_e^2} + \frac{t}{q_e} \quad (5)$$

where k_2 is the rate constant of pseudo-second order chemisorption (g/(mg min)). The constants k_2 and q_2 can be calculated from the intercept and slope of the line obtained by plotting t/qt versus t.
To understand the mechanism of the fluoride adsorption onto fungal biomass, intra-particle diffusion-based mechanism was studied. As per the intra-particle diffusion model, the plot of uptake, qt versus the square root of time ($t^{1/2}$) should be linear if intra-particle diffusion is the rate-controlling step for the adsorption process and if these lines pass through the origin (Aksu, 2005). The intra-particle diffusion equation can be described as in Eq. (6):

$$q_t = k_i t^{1/2} + C \quad (6)$$

where k_i is the intra-particle diffusion rate constant (mg/g min). The Elovich model assumes that the adsorbent surface is energetically heterogeneous and can also describe the chemisorption process (Zhang and Stanforth, 2005). The linearized equation is given by Eq. (7):

$$q_t = \beta \ln(\alpha\beta) + \beta \ln t \quad (7)$$

where, α = sorption rate (mmol/(g min)); β = desorption constant (g/mmol). The Elovich coefficients were computed from the plots q_t versus ln t.

All the four fungal biosorbents followed the pseudo-second-order kinetic model with high R2 values as shown in Table 3. As per this model, the fluoride ions are expected to form covalent bonds by sharing or exchange of electrons with the biosorbent surface and thus fluoride removal takes place due to chemisorptions (Ho and Mckay, 1999). The intra-particle diffusion kinetic model also provides good correlation of the experimental data, which means intra-particle diffusion influences the fluoride adsorption onto biosorbents. The calculated parameters of the model are summarized in Table 3. The Elovich equation provides good agreement with experimental data for *Aspergillus ficuum* SIT-CH-2 and *Aspergillus flavipes* SIT-CH-4 (Table 3), which may be due to the presence of highly heterogeneous surfaces and also it shows that along with surface adsorption chemisorption is also a dominant phenomenon taking place. But, in a highly heterogeneous system along with surface adsorption, chemisorptions, ion exchange, precipitation and intra-particle diffusion are occurring concurrently. However, the correlation coefficients of Elovich equation are lower than those of the pseudo second-order equation and intra-particle diffusion model (Zhang and Stanforth, 2005).

Statistical analysis

Experiments based on the CCD matrix were used to determine the effect of variables: pH (2.0–8.0), initial fluoride concentration (10–100 mg/L), adsorbent dosage (1–10 g/L), and contact time (30-240 min) on the response (Y). Y represents the percentage fluoride biosorption.

Second-order polynomial equations drew the relationship between the independent variables and the response. The regression equation coefficients were evaluated and fitted to a second-order polynomial equation for fluoride removal using fungal strains. The correlations between fluoride removal efficiency (Y) and the four parameters in coded form developed by CCD are represented in Eqs. 8, 9, 10 and 11 for *Penicillium camemberti* SIT-CH-1, *Aspergillus ficuum* SIT-CH-2, *Aspergillus terreus* SIT-CH-3, and *Aspergillus flavipes* SIT-CH-4, respectively. The results of ANOVA for the removal of fluoride ions using fungal biomass are shown in Table 4. The predicted R^2 and the adjusted R^2 are in reasonable agreement and closer to1.0. This confirms that the model fits the experimental data well.

Penicillium camemberti SIT-CH-1:

$$Y = 12.09 - 2.97 * A + 2.03 * B - 7.09 * C + 4.51 * D - 1.71 * AB + 1.63 * AC - 2.5^{-3} * A - 0.42 * BC + 1.74 * BD - 1.52 * CD + 3.56 * A^2 + 1.66 * B^2 - 1.77 * C^2 + 0.81 * D^2 \quad (8)$$

Aspergillus ficuum SIT-CH-2:

$$Y = 12.51 - 0.34 * A + 1.29 * B - 8.98 * C + 2.73 * D + 2.16 * AB - 1.89 * AC + 0.16 * AD - 1.72 * BC + 1.26 * BD - 1.88 * CD + 1.04 * A^2 - 1.61 * B^2 + 5.62 * C^2 - 2.9 * D^2 \quad (9)$$

Aspergillus terreus SIT-CH-3:

$$Y = 12.61 + 0.67 * A + 4.1 * B - 5.16 * C + 1.65 * D - 1.39 * AB - 2.17 * AC + 0.26 * AD + 8.75^{-3} * BC + 0.73 * BD - 0.2 * CD \quad (10)$$

Aspergillus flavipes SIT-CH-4:

$$Y = 5.98 - 3.62 * A + 3.69 * B - 6.81 * C + 0.95 * D - 0.79 * AB - 0.13 * AC + 0.21 * AD - 1.63 * BC + 0.055 * BD - 0.48 * CD + 7.22 * A^2 + 0.97 * B^2 + 3.66 * C^2 - 0.64 * D^2 \quad (11)$$

The interactive effects of two independent variables on the response are displayed in contour plots in Figures 4-7. The pH and biosorbent dosage were determined to be the significant factors with p values greater than 0.0001 for all the four fungal species as they greatly influenced the biosorption of fluoride ions. The biosorption of fluoride concentration and contact time also play a significant role in the biosorption of fluoride ions. The greater removal of fluoride ions with the increase in initial fluoride concentration is because of an increased concentration gradient for the mass transfer of fluoride ions. The increase in contact time helps in greater fluoride removal as there is more time for adsorption to take place and to attain equilibrium conditions. Fungal cell walls mainly contain chitin and amine groups (Troy and Kofer, 1969). The pK (proton dissociation constant) of positively charged acetylamine groups in chitin is 3.5, while amine groups of other biomolecules have pK around 6 (Roberts, 1992). Therefore,

Table 4. ANOVA for the response of percentage fluoride removal

	***Penicillium camemberti* SIT-CH-1**					***Aspergillus ficuum* SIT-CH-2**				
Source	**Sum of Squares**	**df**	**Mean Square**	**F Value**	**p-value Prob > F**	**Sum of Squares**	**df**	**Mean Square**	**F Value**	**p-value Prob > F**
Model	1815.18	14	129.66	118.55	< 0.0001	1990.04	14	142.15	137.99	< 0.0001
A-Initial F⁻ concn	158.66	1	158.66	145.07	< 0.0001	2.05	1	2.05	1.99	0.1783
B-Biosorbent dosage	74.46	1	74.46	68.09	< 0.0001	29.82	1	29.82	28.95	< 0.0001
C-pH	905.26	1	905.26	827.73	< 0.0001	1451.06	1	1451.06	1408.64	< 0.0001
D-contact time	366.32	1	366.32	334.94	< 0.0001	134.11	1	134.11	130.19	< 0.0001
AB	46.72	1	46.72	42.72	< 0.0001	74.47	1	74.47	72.30	< 0.0001
AC	42.58	1	42.58	38.93	< 0.0001	57.30	1	57.30	55.63	< 0.0001
AD	1.000E-004	1	1.000E-004	9.143E-005	0.9925	0.40	1	0.40	0.39	0.5439
BC	2.77	1	2.77	2.53	0.1322	47.42	1	47.42	46.03	< 0.0001
BD	48.44	1	48.44	44.29	< 0.0001	25.54	1	25.54	24.79	0.0002
CD	36.97	1	36.97	33.80	< 0.0001	56.46	1	56.46	54.81	< 0.0001
A^2	32.90	1	32.90	30.08	< 0.0001	2.80	1	2.80	2.72	0.1197
B^2	7.17	1	7.17	6.55	0.0218	6.71	1	6.71	6.52	0.0221
C^2	8.14	1	8.14	7.45	0.0155	81.84	1	81.84	79.45	< 0.0001
D^2	1.69	1	1.69	1.55	0.2323	21.80	1	21.80	21.16	0.0003
Residual	16.41	15	1.09			15.45	15	1.03		
Lack of Fit	10.77	10	1.08	0.96	0.5573	12.80	10	1.28	2.41	0.1714
Pure Error	5.63	5	1.13			2.65	5	0.53		
Cor Total	1831.58	29				2005.49	29			
R-Squared	0.9910					0.9923				
	***Aspergillus terreus* SIT-CH-3**					***Aspergillus flavipes* SIT-CH-4**				
Model	954.27	10	95.43	433.81	< 0.0001	2175.95	14	155.43	158.47	< 0.0001
A-Initial F⁻ concn	8.09	1	8.09	36.79	< 0.0001	235.73	1	235.73	240.35	< 0.0001
B-ads dose	301.95	1	301.95	1372.67	< 0.0001	244.63	1	244.63	249.43	< 0.0001
C-pH	478.60	1	478.60	2175.72	< 0.0001	833.90	1	833.90	850.25	< 0.0001
D-Contact time	48.80	1	48.80	221.82	< 0.0001	16.28	1	16.28	16.60	0.0010
AB	31.08	1	31.08	141.29	< 0.0001	10.02	1	10.02	10.21	0.0060
AC	75.52	1	75.52	343.29	< 0.0001	0.27	1	0.27	0.28	0.6072
AD	1.11	1	1.11	5.06	0.0365	0.69	1	0.69	0.70	0.4151
BC	1.225E-003	1	1.225E-003	5.569E-003	0.9413	42.64	1	42.64	43.48	< 0.0001
BD	8.47	1	8.47	38.50	< 0.0001	0.048	1	0.048	0.049	0.8272
CD	0.65	1	0.65	2.95	0.1024	3.74	1	3.74	3.82	0.0696
A^2	4.18	19	0.22			135.22	1	135.22	137.87	< 0.0001
B^2	2.55	14	0.18	0.56	0.8191	2.44	1	2.44	2.48	0.1358
C^2	1.63	5	0.33			34.72	1	34.72	35.40	< 0.0001
D^2	958.45	29				1.06	1	1.06	1.08	0.3151
Residual	0.9956					14.71	15	0.98		
Lack of Fit	954.27	10	95.43	433.81	< 0.0001	13.24	10	1.32	4.51	0.0551
Pure Error	8.09	1	8.09	36.79	< 0.0001	1.47	5	0.29		
Cor Total	301.95	1	301.95	1372.67	< 0.0001	2190.66	29			
R-Squared	478.60	1	478.60	2175.72	< 0.0001	0.9933				

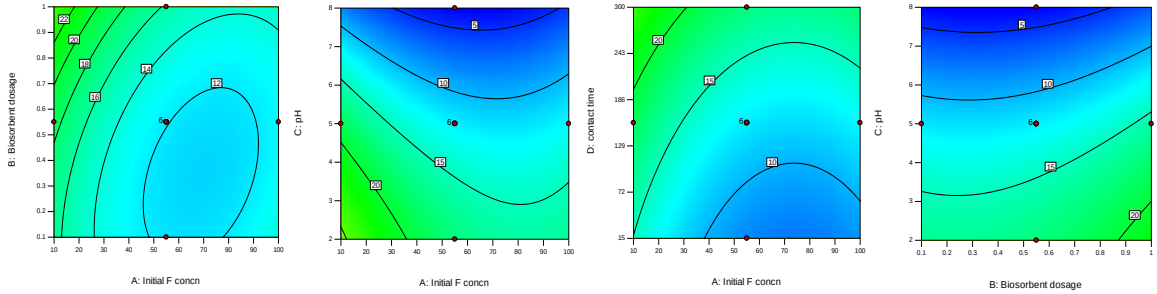

Figure 4. Contour plots of fluoride removal using *Penicillium camemberti* SIT-CH-1 versus the effect of four variables (effect of A: initial concentration, B: adsorbent dose, C: pH, D: contact time)

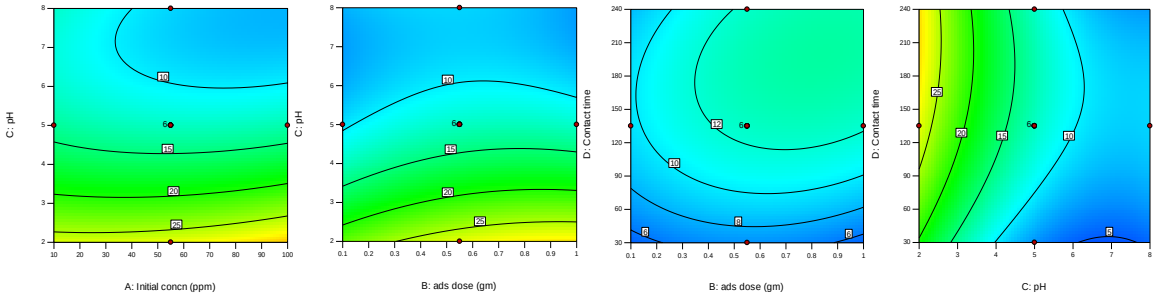

Figure 5. Contour plots of fluoride removal using *Aspergillus ficuum* SIT-CH-2 versus the effect of four variables (effect of A: initial concentration, B: adsorbent dose, C: pH, D: contact time)

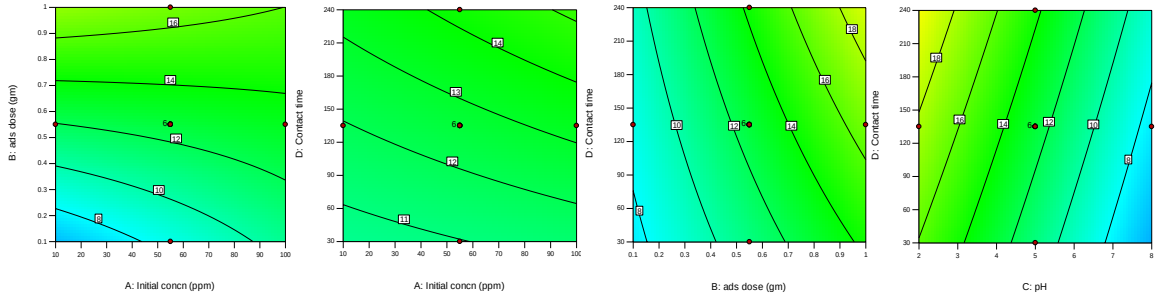

Figure 6. Contour plots of fluoride removal using *Aspergillus terreus* SIT-CH-3 versus the effect of four variables (effect of A: initial concentration, B: adsorbent dose, C: pH, D: contact time)

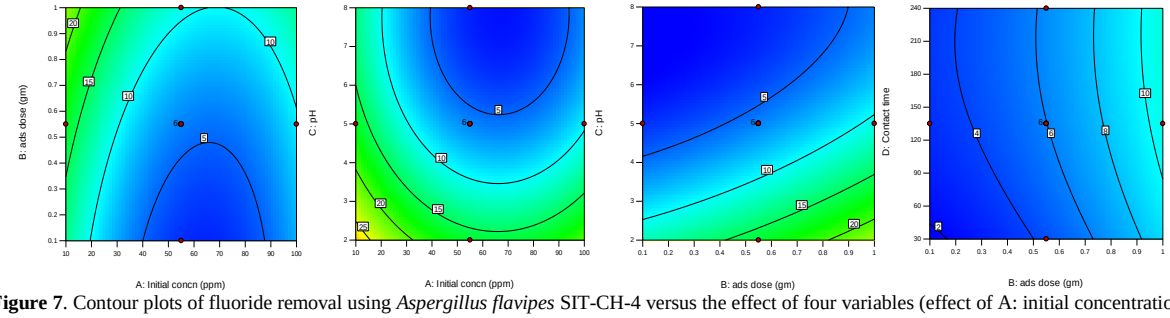

Figure 7. Contour plots of fluoride removal using *Aspergillus flavipes* SIT-CH-4 versus the effect of four variables (effect of A: initial concentration, B: adsorbent dose, C: pH, D: contact time)

most of the amine groups on the fungal biomass could be positively charged by protons at pH 2.0. This may be the reason for the increased biosorption of fluoride ions at lower pH. There may be compositional differences among the cell walls, as well as varying binding mechanisms involved for different fungal species (Sheng et al. 2004; Naja et al. 2010).

Conclusion

The biosorption process offers an eco-friendly, safe and economical technology for the fluoride treatment of water. The FTIR analysis proposed that the H¯, N¯, and O functional groups present on the biomass are probably involved in fluoride biosorption on fungal biomass. The pseudo-second-order kinetic model showed the best fit for all the four fungal species for fluoride biosorption. This again is a proof that there is single layer formation of fluoride onto the fungal biosorbents and that the fluoride ions form covalent bonds by sharing or exchange of electrons with the biosorbent surface and hence fluoride removal takes place. The maximum fluoride uptake capacity is found to be >2.5 mg/g for all the four fungal species.

Acknowledgment

The authors would like to thank the Director, Principal, and Management of Siddaganga Institute of Technology, Tumkur for their support.

References

Aksu Z (2005) Application of biosorption for the removal of organic pollutants: a review, Process Biochemistry, 40: 997.

Amin F, Talpur FN, Balouch A, Surhio MA, Bhutto MA (2015) Biosorption of fluoride from aqueous solution by white—rot fungus Pleurotus eryngii ATCC 90888, Environmental Nanotechnology, Monitoring & Management, 3: 30.

Barnett HL, Hunter BB, (1998) Illustrated genera of imperfect fungi. APS Press, St. Paul Minnesota, USA.

Harley JP, Prescott LM (1993) Basic laboratory and culture techniques. In: Laboratory exercises in microbiology. 2nd Ed., W.C. Brown Publishers, Dubuque, pp. 14-46.

Ho YS, Mckay G (1999) Pseudo-second order model for sorption process, Process Biochemistry, 34: 451.

Lagergren S (1898) About the theory of so called adsorption of soluble substances. Vetenskapsad Handl., 24: 1.

Mamatha P, Sudhakar Rao M (2010) Geochemistry of fluoride rich groundwater in Kolar and Tumkur Districts of Karnataka, Environ. Earth Sci., 61: 131.

Myers RH, Montgomery DC (2002) Response Surface Methodology. 2nd Ed., New York: John Wiley and Sons.

Naja GM, Murphy V, Volesky B (2010) Biosorption, Metals. In: Encyclopedia of Industrial Biotechnology, 1: 29.

Navya PN, Pushpa SM, (2013) Production, statistical optimization and application of endoglucanase from Rhizopus stolonifer utilizing coffee husk, Bioprocess and Biosystems, 36(8): 1115.

Purvis OW, Halls C (1996) A review of lichens in metal-enriched environments. Lichenologist, 28, 571-601.

Roberts GAF, (1992) Chitin Chemistry, Macmillan, London, UK. pp 204-206.

Sheng PX, Ting YP, Chen JP Hong L, (2004) Sorption of lead, copper, cadmium, zinc, and nickel by marine algal biomass: characterization of biosorptive capacity and investigation of mechanisms. J. Colloid Interface Sci., 275, 1, 131.

Smith BC (1998) Infrared Spectral Interpretation: A Systematic Approach, (1st ed.) CRC Press, London.

Troy FA, Koffler H. (1969) The chemistry and molecular architecture of the cell walls of Penicillium chrysogenum, J. Biol. Chem., 244(20): 5563.

Volesky B (2001) Detoxification of metal-bearing effluents: biosorption for the next century. Hydrometallurgy, 59: 203.

Volesky B, Holan ZR (1995) Biosorption of heavy metals. Biotechnol. Prog., 11, 235.

Vu VH, Pham TA, Kim K, (2009) Fungal strain improvement for cellulase production using repeated and sequential mutagenesis. Mycobiol., 37: 267.

WHO 2008. Guidelines for Drinking - Water Quality, 3rd Ed., Incorporating the first and second addenda, Vol. 1, World Health Organization (WHO): Geneva, Switzerland: WHO Press. http://www.who.int/water_sanitation_health/dwq/fulltext.pdf

Zhang J, Stanforth R (2005) Slow adsorption reaction between arsenic species and goethite (α-FeOOH): diffusion or heterogeneous surface reaction control, Langmuir, 21: 2895.